J. Fluid Mech. (1968), *vol.* 32, *part* 1, *pp.* 29–53
Printed in Great Britain

On the propulsion efficiency of swimming flexible hydrofoils of finite thickness

By J. P. ULDRICK

Engineering Department, U.S. Naval Academy, Annapolis, Maryland, U.S.A.

(Received 3 April 1967 and in revised form 27 October 1967)

This paper presents some recent theoretical results on the energy exchange between a swimming flexible two-dimensional hydrofoil of finite profile thickness and the inviscid incompressible fluid in which the body swims. The rate at which kinetic energy is transferred to the fluid by the undulating hydrofoil, the power required to maintain the prescribed motion, and the resulting power available for propulsion are calculated in terms of the thickness to chord ratio and the displacement and rate of displacement of the hydrofoil. With a small unsteady perturbation theory, the analysis is decomposed to show separately the effects of the circulatory and non-circulatory flows, both depending on the first-order terms of the unsteady perturbation velocity components. In addition, an analysis is presented showing the effect of the non-linear unsteady pressure distribution on the surface of the hydrofoil. Contrary to what might be expected, this latter effect is of the same order of magnitude for a thick rounded-nose profile as for the flat plate where the effect is concentrated at the sharp leading edge and is related to the so-called suction force. However, except for small values of the reduced frequency, the non-linear contribution is negligible in comparison with the linear contribution.

New functions associated with the retarded flow in the wake are introduced and special techniques for their solution are presented, these being related to Theodorsen's function of unsteady airfoil theory for the special case of the undulating flat plate.

The numerical results reveal that the kinetic energy imparted to the fluid, the power required to maintain the motion, and the resulting propulsive power, follow closely those of an infinitesimal model for small values of the reduced frequency of oscillation, but diverge somewhat from the classical thin plate analysis for large reduced frequencies. Of particular interest is the fact that a very large percentage of the power required to maintain the motion is used in the generation of the wake, whereas a very small percentage of the power available for propulsion comes from the wake. This indicates that, if some mechanism could be devised to control the wake, very high swimming efficiencies could be attained. Fish, in all probability, have been succeeding in doing this for millions of years.

1. Introduction

During the past two decades considerable interest has developed between researchers in biology and in engineering hydrodynamics concerning the manner of manoeuvrability of various types of aquatic animals. Gray's work (1936, 1948,

1957), in which he calculated the power dissipated by skin friction of a dolphin swimming at constant speed, was the primary stimulus for much of this interest.

Taylor (1951, 1952*a*) paved the way for new problems in hydrodynamics with a study concerning the action of moving cylindrical tails in propelling microscopic organisms in a viscous fluid, in which he assumed the tail of the organism to be a flexible cylinder which is distorted by waves of lateral displacement propagated along its length. He assumed that the viscous forces played the leading role in propelling the organism. In a subsequent study Taylor (1952*b*) investigated the swimming of long animals such as snakes, eels, and marine worms by considering the equilibrium of a flexible cylinder immersed in water when waves of bending of constant amplitude travel down it at constant speed.

As another approach to the problem of propulsion of sea animals, Siekmann (1963*a*) discussed the hydrodynamics and propulsive properties when a jet of fluid is ejected from the opening of a tube.

Lighthill (1960*a*) discussed the hydrodynamics of fish propulsion at the forty-eighth Wilbur Wright memorial lecture, and in a later publication (1960*b*) he considered the swimming of slender fish in which he employed as a model a slender cylindrical snake-like configuration immersed in a uniform flow field directed along the stretched-straight configuration of the model. His theory goes back to Munk's (1924) work on flow about airships.

All of the above studies dealt with a three-dimensional axisymmetric-type flow problem.

Several investigators have discussed the propulsive forces generated by an undulating flexible plate of infinitesimal thickness and infinite aspect ratio in two-dimensional flow. Each of these investigators assumed that the thrust was generated by small time-dependent lateral displacements which are in the form of waves of displacement that pass down the chord of the plate from the leading edge to determine the forces acting on the plate. Siekmann (1962, 1963*b*) used the unsteady airfoil theory developed by Schwarz (1940) and Küssner & Schwarz (1940) where the thin plate and its wake are replaced by a vortex distribution of fluctuating strength. Smith & Stone (1961) considered the same physical problem as Wu (1961) and Siekmann (1962, 1963*b*) where they represented the plate in elliptic cylindrical co-ordinates. Smith & Stone satisfy the unsteady boundary conditions by solving the Laplace equation for the velocity potential and satisfy the Kutta–Joukowski hypothesis of smooth attached flow at the sharp tail by adding a circulation around the plate of fluctuating strength such that the net induced unsteady velocity at the tail is finite for all time. However, Smith & Stone failed to consider the entire wake and, as such, their theory does not agree with Wu's (1961) and Siekmann's (1962, 1963*b*) theories. Pao & Siekmann (1964) corrected the Smith–Stone theory to include the wake effect.

Bonthron & Fejer (1962) studied the two-dimensional problem of fish locomotion by employing as a model three infinitely thin rigid plates hinged together where both rotational and translational oscillations were imposed upon the plates. They used Theodorsen's (1934) theory for a system of finite degrees of freedom and solved the dynamic equilibrium equation by carefully balancing the side forces for a freely swimming body.

Uldrick & Siekmann (1964) have considered the swimming of a two-dimensional model possessing a finite thickness and have found that the available time average thrust decreases with increasingly thick profiles. They made no attempt to calculate the energy dissipated in the body's wake or the power required to maintain the motion. Moreover, Uldrick & Siekmann's theory is not complete since they linearized their problem by assuming a very small, but finite, thickness. Their theory is modelled after Küssner & Gorup's (1960) theory of unsteady flow about an airfoil of finite thickness.

All of the above studies were purely theoretical in nature.

Kelly (1961) measured experimentally the propulsive forces produced in an undulating, thin two-dimensional plate and found that the theory developed by Siekmann (1962, 1963*b*) and Wu (1961) was in some agreement with experimental evidence when allowance was made for skin friction.

Recently, Kelly & Bowlus (1963) made an experimental investigation of the swimming of hinged hydrofoils. The purpose of their study was to examine a few of the intermediate cases between the completely flexible hydrofoil and the completely rigid one. They chose a NACA symmetric airfoil no. 63009 as a model for the stretched-straight fish and measured the thrust generated by single-hinged and double-hinged hydrofoils undergoing prescribed vertical oscillations (heaving and pitching). Kelly & Bowlus made no attempt at assessing the effect of body thickness on the propulsive force generated by the controlled motion of the hydrofoil.

2. General mathematical and physical formulation of the problem

As a starting-point in the formulation, the general theory developed by Uldrick & Siekmann (1964) will be employed.

To fix ideas, we choose a cartesian co-ordinate system (x', y') fixed relative to the fluid at infinity such that the forward velocity U of the hydrofoil is along the negative x'-axis.

By the Galilean transformation

$$x = x' + Ut + \text{const.}, \quad y = y',$$

the motion is referred to a co-ordinate system (x, y) fixed at the hydrofoil such that the nose is located at $x = -L$ and the tail at $x = L$. Clearly, for a constant forward velocity U, both reference frames are Newtonian; thus, either system can be used to calculate the pressure distribution on the body or, ultimately, the lift, moment, and drag experienced by the body.

We will employ the co-ordinate system (x, y) fixed at the hydrofoil to calculate the pressure distribution.

Consider the symmetric profile with length $2L$ as shown in figure 1. This we call the stretched-straight configuration. It has a rounded leading edge and a sharp trailing edge.

Now, let us immerse this configuration in an incompressible irrotational flow field such that the flow is symmetrical around the body where the flow is along the positive x-axis as shown in figure 1. Since the flow is assumed to be irrotational, we use complex variable theory to determine the flow properties around

this body. This is accomplished by determining the flow field around a circular cylinder and then by a conformal transformation calculating the flow field around the symmetric body. To describe the flow field, we employ the complex velocity potential method.

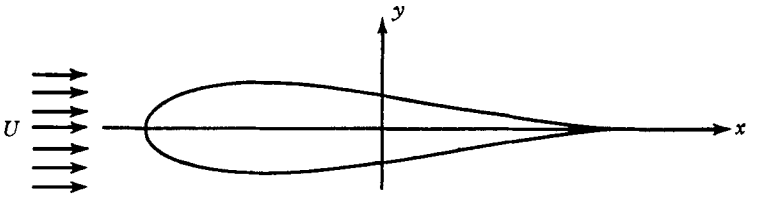

FIGURE 1a. Profile plane ($z = x+iy$ plane).

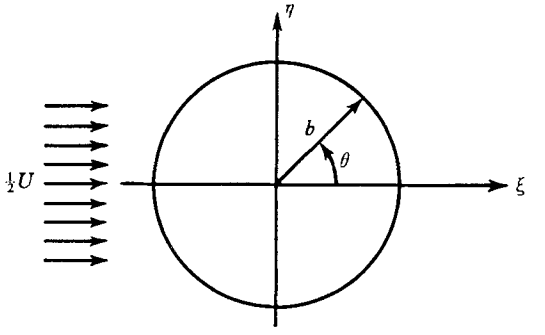

FIGURE 1b. Circle plane ($\zeta = \xi+i\eta$ plane).

We denote the complex space variables in the circle plane by $\zeta = \xi+i\eta$, as shown in figure 1b.

From the circle theorem the complex potential $F_0(\zeta)$ is easily seen to be

$$F_0(\zeta) = \frac{U}{2}\left(\zeta+\frac{b^2}{\zeta}\right), \tag{2.1}$$

where b is the radius of the circle. The free-stream velocity in the ζ-plane is taken to be $U/2$ for convenience.

As a model for the stretched-straight configuration, we employ a symmetric Joukowski profile given by

$$z = f(\zeta) = \frac{1}{2}\left[\zeta-\epsilon+\frac{(b-\epsilon)^2}{\zeta-\epsilon}\right]+E, \tag{2.2}$$

where ϵ is a small positive quantity ($0 \leqslant \epsilon < b$) representing a measure of the thickness, and E is a real quantity which locates the head at $x = -L$ and the tail at $x = L$.

The unsteady motion of the hydrofoil is chosen to simulate that of certain sea animals. We express this displacement in general complex time and space as

$$D(z,t) = iH^*(x)\,e^{j\omega t}, \tag{2.3}$$

where $j = \sqrt{-1}$, which is not to be confused with the space imaginary unit i, and $H^*(x)$ is complex with respect to j. Remember in the final analysis we must take the real part in the complex time quantities for physical interpretation.

According to Uldrick & Siekmann (1964) the linearized unsteady boundary condition for the fluid velocity is

$$\frac{dz}{dt} = \frac{\partial D}{\partial t} + \frac{\overline{dF_0}}{dz}\frac{\partial D}{\partial z}, \tag{2.4}$$

and the corresponding velocity of a fluid particle in a normal direction on the circle is

$$\hat{q}_r(\vartheta, t) = UG(\vartheta)\, e^{j\omega t},\dagger \tag{2.5}$$

where

$$G(\vartheta) = -R_i \frac{1}{b^2}\overline{\left\{\frac{dz}{d\vartheta}\left(j\sigma H_1^*(\vartheta) - \frac{\sin\vartheta}{|f'(b\,e^{i\vartheta})|^2}\frac{dH_1^*(\vartheta)}{d\vartheta}\right)\right\}}_{z=f(b\,e^{i\vartheta})} \tag{2.6}$$

in which R_i denotes the space real part operator, $\sigma = \omega b/U$ is the reduced frequency, and $H_1^*(\theta) = H^*(x)$. For the symmetric body here under consideration it can be shown that $G(\vartheta)$ is an odd function which we expand in a Fourier series as

$$G(\vartheta) = 2\sum_{n=1}^{\infty} P_n \sin n\vartheta = 2\sum_{n=1}^{\infty} \frac{1}{b^2}[b_n - c_n]\sin n\vartheta, \tag{2.7}$$

where the b_n and c_n can be calculated from equation (2.6) by the Fourier inversion formula. It should be noted that these coefficients are complex with respect to j.

The boundary condition on the circle can be satisfied by a source distribution on the boundary of the circle. From the basic definition of a source, it follows that

$$F_1(\zeta, t) = \frac{Ue^{j\omega t}}{2\pi}\int_0^{2\pi} G(\vartheta)\log(\zeta - b\,e^{i\vartheta})^2 b\,d\vartheta. \tag{2.8}$$

Due to the presence of a sharp tail, the unsteady velocity there resulting from F_1 will be infinite. Thus, as in unsteady airfoil theory, we introduce a sheet of distributed vortices along the wake streamline of the steady flow with a distribution of counter-image vortices on the interior of the circle such that the corresponding induced velocity at the sharp tail by these vortices will cancel for all time that due to the source potential. Furthermore, we assume that each vortex element moves downstream with the local velocity of the steady state flow and does not decay. Under these conditions the circulatory potential can be written as

$$F_2(\zeta, t) = \frac{i\gamma_0}{2\pi}\int_b^{\infty} \log\frac{\zeta - \xi_0}{\zeta - b^2/\xi_0}\, e^{j\omega(t-\tau)} f'(\xi_0)\, d\xi_0, \tag{2.9}$$

where

$$\gamma_0 = \frac{2U\sum_{n=1}^{\infty} P_n}{\dfrac{1}{2\pi b}\displaystyle\int_b^{\infty}\frac{\xi_0 + b}{\xi_0 - b}\, e^{-j\omega\tau} f'(\xi_0)\, d\xi_0} \tag{2.10}$$

and

$$\tau = \int_{x_\tau}^{x_0} \frac{dx_0}{\overline{F}_0'(\xi_0)/f'(\xi_0)} = \int_b^{\xi_0} \frac{|f'(\xi_0)|^2}{\overline{F}_0'(\xi_0)}\, d\xi_0 \tag{2.11}$$

is the age of the vortex element situated at $x_0 = f(\xi_0)$.

Finally, with the small perturbation theory we have

$$F = F_0(\zeta) + F_1(\zeta, t) + F_2(\zeta, t) \tag{2.12}$$

and

$$w = \frac{\partial F}{\partial z} = u - iv. \tag{2.13}$$

† Quantities in the circle plane are denoted by a circumflex. A bar over a function denotes its complex conjugate.

3. Pressure distribution on the surface of the body

From the unsteady Bernoulli equation, we have

$$p = p_0 - \rho\left(\frac{\partial \phi}{\partial t} + \tfrac{1}{2}q^2\right), \tag{3.1}$$

where p_0 is the pressure far upstream from the body, which is taken to be constant, ϕ is the velocity potential, which in our case is the real part in the space imaginary unit i of the complex potential F, and q is the speed of the considered fluid particle. Substituting (2.12) into (3.1), we get for the unsteady pressure distribution on the body

$$\Pi(\vartheta, t) = -\rho R_i\left(\frac{\partial F}{\partial t} + \frac{1}{2|f'|^2}\frac{\overline{\partial F}}{\partial \zeta}\frac{\partial F}{\partial \zeta}\right)_{\zeta = b e^{i\vartheta}}. \tag{3.2}$$

It is convenient to decompose this distribution into three parts as follows:

$$\Pi(\vartheta, t) = \Pi_1(\vartheta, t) + \Pi_2(\vartheta, t) + \Pi_3(\vartheta, t), \tag{3.3}$$

where

$$\Pi_1(\vartheta, t) = -\rho R_i\left(\frac{\partial}{\partial t} + \frac{\overline{F_0'(\zeta)}}{|f'(\zeta)|^2}\frac{\partial}{\partial \zeta}\right) F_1(\zeta, t)\Big|_{\zeta = b e^{i\vartheta}}, \tag{3.3a}$$

$$\Pi_2(\vartheta, t) = -\rho R_i\left(\frac{\partial}{\partial t} + \frac{\overline{F_0'(\zeta)}}{|f'(\zeta)|^2}\frac{\partial}{\partial \zeta}\right) F_2(\zeta, t)\Big|_{\zeta = b e^{i\vartheta}}, \tag{3.3b}$$

and

$$\Pi_3(\vartheta, t) = -\frac{\rho}{2} R_i\left[\frac{\overline{\partial(F_1 + F_2)}}{\partial \zeta}\frac{\partial(F + F_2)}{\partial \zeta}\frac{1}{|f'(\zeta)|^2}\right]_{\zeta = b e^{i\vartheta}}. \tag{3.3c}$$

It should be noted that Π_1 and Π_2 are of first order in the unsteady velocity components, whereas Π_3 is of second order in the perturbation velocity. In the small perturbation theory usually the non-linear terms are neglected in the analysis. However, as will be shown in what follows, the effect of the non-linear terms is of the same order of magnitude as that of the linear terms, and hence cannot be neglected.

By substituting (2.7) and (2.8) into (3.3a) we find, after some lengthy analyses, that the non-circulatory pressure distribution becomes

$$\Pi_1(\theta, t) = 2\rho U^2 e^{j\omega t}\sum_{n=1}^{\infty} P_n\left[j\sigma\frac{\sin n\theta}{n} - \frac{\sin\theta}{|f'(b e^{i\theta})|^2}\cos n\theta\right]. \tag{3.4}$$

The circulatory pressure distribution Π_2 on the body can be found as follows. First, we note that the time variation in F_2 is due entirely to the movement of the vortex element, i.e.

$$\frac{\partial F_2}{\partial t} = \frac{\partial F_2}{\partial \xi_0}\frac{d\xi_0}{dx_0}\frac{dx_0}{dt} = \frac{\overline{F'(\xi_0)}}{|f'(\xi_0)|^2}\frac{\partial F_2}{\partial \xi_0}. \tag{3.5}$$

Using the last result and (2.9) in (3.3b) it follows that the pressure distribution due to the coupling of the vortex sheet and the free stream is

$$\Pi_2(\theta, t) = \rho U^2 2\sum_{n=1}^{\infty} P_n \mathscr{W} e^{j\omega t}, \tag{3.6}$$

where $\mathscr{W} = \frac{1}{UbW_0}\int_b^\infty \left[\frac{\overline{F_0'(\xi_0)}}{|f'(\xi_0)|^2}\frac{2b^2\sin\theta}{b^2+\xi_0^2-2b\xi_0\cos\theta} + \frac{U\sin\theta}{|f'(be^{i\theta})|^2}\frac{\xi_0^2-b^2}{b^2+\xi_0^2-2b\xi_0\cos\theta}\right] \times e^{-j\omega\tau}f'(\xi_0)\,d\xi_0, \quad (3.7)$

in which
$$W_0 = \frac{1}{b}\int_b^\infty \frac{\xi_0+b}{\xi_0-b}e^{-j\omega\tau}f'(\xi_0)\,d\xi_0. \quad (3.8)$$

Finally, the unsteady pressure Π_3 resulting from the non-linear terms in the Bernoulli equation (3.3*c*) can be expressed in terms of the unsteady velocities as

$$\Pi_3(\theta,t) = -\frac{\rho}{2}(\hat{w}_1+\hat{w}_2)\overline{(\hat{w}_1+\hat{w}_2)}\frac{1}{|f'(be^{i\theta})|^2}, \quad (3.9)$$

where it evolves from equations (2.8), (2.9) and (2.13) that

$$\hat{w}_1(\theta,t) = iUe^{j\omega t}e^{-i\theta}2\sum_{n=1}^{\infty}P_n\cos n\theta \quad (3.10)$$

and
$$\hat{w}_2(\theta,t) = \frac{-i\gamma_0 e^{-i\theta}e^{j\omega t}}{2\pi b}\int_b^\infty \frac{\xi_0^2-b^2}{b^2+\xi_0^2-2b\xi_0\cos\theta}e^{-j\omega\tau}f'(\xi_0)\,d\xi_0. \quad (3.11)$$

Geometrically it can be seen that the magnitude of $\hat{w}_2(\theta,t)$ is an even function of θ and is proportional to the integral expression in (3.11). Thus we write

$$\hat{w}_2(\theta,t) = \frac{-i\gamma_0 e^{-i\theta}e^{j\omega t}}{2\pi b}\left(W_{20}+2\sum_{n=1}^{\infty}W_{2n}\cos n\theta\right), \quad (3.12)$$

where, by the Fourier inversion formula, it follows that

$$W_{2n} = \frac{1}{b}\int_b^\infty \left(\frac{\xi_0}{b}\right)^{-n}e^{-j\omega\tau}f'(\xi_0)\,d\xi_0. \quad (3.13)$$

Finally, by substituting (2.10) and (3.8) into (3.12), there results

$$\hat{w}_2(\theta,t) = -ie^{-i\theta}U2\sum_{m=1}^{\infty}P_m e^{j\omega t}\left[V_0+2\sum_{n=1}^{\infty}V_n\cos n\theta\right], \quad (3.14)$$

in which we defined the ratio
$$V_n = W_{2n}/W_0 \quad (3.15)$$

and refer to it as a wake function. Clearly, the coefficients V_n are complex in the time imaginary unit j and are functions of the reduced frequency and mapping function $z = f(\zeta)$ only.

From (3.10) and (3.14) we obtain

$$\hat{w}_1+\hat{w}_2 = -ie^{-i\theta}Ue^{j\omega t}\left[V_0\left(2\sum_{m=1}^{\infty}P_m\right)+2\sum_{n=1}^{\infty}\left(V_n\left(2\sum_{m=1}^{\infty}P_m\right)-P_n\right)\cos n\theta\right], \quad (3.16)$$

and thus, from (3.3*c*), $\Pi_3(\theta,t)$ can be calculated. It should be pointed out that the Kutta condition places constraints

$$V_0+2\sum_{n=1}^{\infty}V_n = 1 \quad (3.17)$$

on the wake functions.

Inspection of (3.16) and (3.3c) indicates that $\Pi_3(\theta, t)$ is an even function of θ which can be expressed in a Fourier cosine series.

4. Formation of energy transfer concepts

In order to calculate the efficiency of propulsion, we need to determine the energy dissipated in the fluid during some time interval of motion. For an incompressible inviscid fluid, Serrin (1959) gives the rate of change of kinetic energy in a material volume of an incompressible inviscid fluid with constant body forces as

$$\frac{d}{dt}\iiint_{\mathscr{V}(t)} \tfrac{1}{2}\rho \mathbf{V}.\mathbf{V}\, d\tau = -\oiint_{\mathscr{S}(t)} p\mathbf{V}.\mathbf{n}\, ds, \tag{4.1}$$

where $\mathbf{V}$ is the velocity of the fluid particle contained in the element of volume $d\tau$ referred to the co-ordinate systems fixed in the fluid at infinity; d/dt denotes the material derivative with respect to time; $\mathscr{V}$ is the material volume, i.e. the entire volume exterior to the hydrofoil; $\mathscr{S}$ is the surface enclosing $\mathscr{V}$; $\mathbf{n}$ is the outward unit normal vector; and ds is the element of surface area.

Now at any instant of time the kinetic energy of the fluid is

$$E(t) = \iiint_{\mathscr{V}(t)} \tfrac{1}{2}\rho \mathbf{V}.\mathbf{V}\, d\tau. \tag{4.2}$$

We wish to determine the kinetic energy generated by the motion of the hydrofoil during some period of time, say the period of one oscillation $T_0 = 2\pi/\omega$. Thus, from (4.1) and (4.2) it develops that the time average increase in kinetic energy generated in the fluid by the undulating hydrofoil is

$$\langle E \rangle = -\frac{1}{T_0}\int_0^{T_0} \oiint_{\mathscr{S}(t)} p\mathbf{V}.\mathbf{n}\, ds\, dt. \tag{4.3}$$

Next, we must analyse the integral on the right of (4.3). Since $\mathscr{S}$ is a material surface, only the unsteady pressure distribution contributes to this surface integral. We decompose $\mathscr{S}$ into a surface $\mathscr{S}_\infty$ and $\mathscr{S}_B$, a cylindrical surface with a radius $R \to \infty$ from the body and the surface of the body, respectively. The surface $\mathscr{S}_\infty$ can be taken at a sufficiently large distance from the disturbing body that the surface integral on $\mathscr{S}_\infty$ vanishes. Thus, we have

$$E(t) = -\oiint_{\mathscr{S}_B} \mathbf{n}.p\mathbf{V}\, ds. \tag{4.4}$$

In order to avoid a cumbersome notation, we first evaluate the surface integral, which can be written in our complex notation as

$$E(t) = -R_i \oiint_{\mathscr{S}_B} i\frac{dz}{|dz|} R_j\{\Pi_1 + \Pi_2 + \Pi_3\} R_j\left(\frac{\partial F}{\partial z} - U\right)|dz|\Big|_{z=f(b\,e^{i\theta})}. \tag{4.5}$$

However, on $\mathscr{S}_B$ it can be shown that

$$R_i\left\{i\frac{dz}{|dz|} R_i \frac{\partial F}{\partial z}\right\}|dz|\Big|_{z=f(b\,e^{i\theta})} = -R_j \hat{q}_r b\, d\theta. \tag{4.6}$$

Employing this last formula and (2.5) to (2.7), equation (4.5) becomes

$$E(t) = U\frac{1}{b}\int_0^{2\pi} R_j(\Pi_1+\Pi_2+\Pi_3)R_j 2\sum_{n=1}^{\infty} j\sigma b_n e^{j\omega t}\sin n\theta\, d\theta$$
$$- U\frac{1}{b}\int_0^{2\pi} R_j(\Pi_1+\Pi_2+\Pi_3)R_j 2\sum_{n=1}^{\infty} c_n e^{j\omega t}\sin n\theta\, d\theta$$
$$+ UR_i i\iint_{\mathscr{S}_B} R_j(\Pi_1+\Pi_2+\Pi_3)\,dz. \tag{4.7}$$

By a careful analysis of the first term in (4.7), it can be seen that this is simply the power required to drive the hydrofoil, i.e.

$$P(t) = \frac{U}{b}\int_0^{2\pi} R_j(\Pi_1+\Pi_2+\Pi_3)R_j 2\sum_{n=1}^{\infty} j\sigma b_n e^{j\omega t}\sin n\theta\, d\theta. \tag{4.8}$$

The remaining terms in (4.7) may be thought of as the power put into the fluid by virtue of the hydrofoil's movement through a still fluid, which we denote by

$$W(t) = -\frac{U}{b}\int_0^{2\pi} R_j(\Pi_1+\Pi_2+\Pi_3)R_j 2\sum_{n=1}^{\infty} c_n e^{j\omega t}\sin n\theta\, d\theta$$
$$+ UR_i i\iint_{\mathscr{S}_B} R_j(\Pi_1+\Pi_2+\Pi_3)\,dz. \tag{4.9}$$

It should be noted that, if $W(t)$ is positive, energy is being put into the fluid by this power term. On the other hand, if $W(t)$ is negative, energy is being extracted from the fluid by the body and, as such, represents the power capable of propelling the hydrofoil. Thus, we define the power of propulsion as $T(t)U = -W(t) = \mathscr{P}(t)$, where $T(t)$ is a thrust force acting on the body in the direction of the forward motion of the body.

5. Power required to drive the hydrofoil

The power input is given by (4.8). We introduce the notation

$$\left.\begin{aligned} b_n e^{j\omega t} &= \bar{b}'_n + j\bar{b}''_n = (b'_n + jb''_n)e^{j\omega t},\\ P_n e^{j\omega t} &= \bar{P}'_n + j\bar{P}''_n = (P'_n + jP''_n)e^{j\omega t},\end{aligned}\right\} \tag{5.1}$$

and similar relationships for the other coefficients.

Thus, from (5.1) and (4.8) there follows

$$P(t) = -\sigma\frac{U}{b}\int_0^{2\pi} R_j\{\Pi_1+\Pi_2+\Pi_3\}2\sum_{n=1}^{\infty}\bar{b}''_n\sin n\theta\, d\theta. \tag{5.2}$$

It is convenient and instructive to compute the power in three parts depending upon the pressure Π_1, Π_2 and Π_3. By employing (3.4) and (5.1) and by introducing the relation

$$\beta_0 + 2\sum_{n=1}^{\infty}\beta_n\cos n\theta = \frac{\sin\theta}{|f'(be^{i\theta})|^2}2\sum_{n=1}^{\infty} b_n\sin n\theta, \tag{5.3}$$

we find the power required to generate the non-circulatory flow is

$$P_1 = 2\pi\rho U^3\frac{\sigma}{b}\left[2\sum_{n=1}^{\infty}\left(\sigma\frac{\bar{P}''_n\bar{b}''_n}{n} + \bar{P}''_n\bar{\beta}''_n\right)\right]. \tag{5.4}$$

Next, the power required to produce the wake is calculated by (3.6) and (5.2) as

$$P_2 = -\omega b R_j\left\{\rho U^2 2 \sum_{m=1}^{\infty} P_m e^{j\omega t} \int_0^{2\pi} \mathscr{W} 2 \sum_{n=1}^{\infty} \bar{b}_n'' \sin n\theta \, d\theta\right\}. \tag{5.5}$$

By employing (3.7) and (5.5) and performing the indicated integrations, we obtain

$$P_2(t) = -2\pi\rho U^3 \frac{\sigma}{b} R_j\left\{2 \sum_{m=1}^{\infty} P_m e^{j\omega t} \frac{2 \sum_{n=1}^{\infty} \bar{b}_n'' W_{1n} + \bar{\beta}_0'' W_{20} + 2 \sum_{n=1}^{\infty} \bar{\beta}_n'' W_{2n}}{W_0}\right\}, \tag{5.6}$$

where

$$W_{1n} = \frac{1}{b\bar{U}} \int_b^{\infty} \frac{\bar{F}_0'(\xi_0)}{f'(\xi_0)} \left(\frac{\xi_0}{b}\right)^{-(n+1)} e^{-j\omega\tau} d\xi_0 \tag{5.7}$$

and W_{2n} is given by (3.13).

We introduce the notation

$$W_0 = W_0' + jW_0'', \quad W_{1n} = W_{1n}' + jW_{1n}'', \quad W_{2n} = W_{2n}' + jW_{2n}'', \tag{5.8}$$

and the ratios

$$U_n = U_n' + jU_n'' = W_{1n}/W_0 \quad \text{and} \quad V_n = V_n' + jV_n'' = W_{2n}/W_0. \tag{5.9}$$

By employing these notations, (5.6) becomes

$$\begin{aligned} P_2(t) = -2\pi\rho U^3 \frac{\sigma}{b}\Bigg\{2 \sum_{m=1}^{\infty} \bar{P}_m'\Bigg[2 \sum_{n=1}^{\infty} \bar{b}_n'' U_n' + \bar{\beta}_0'' V_0' + 2 \sum_{n=1}^{\infty} \bar{\beta}_n'' V_n'\Bigg] \\ - 2 \sum_{m=1}^{\infty} \bar{P}_m''\Bigg[2 \sum_{n=1}^{\infty} \bar{b}_n'' U_n'' + \bar{\beta}_0'' V_0'' + 2 \sum_{n=1}^{\infty} \bar{\beta}_n'' V_n''\Bigg]\Bigg\}. \end{aligned} \tag{5.10}$$

The power P_3 can be calculated in a similar manner by using (5.2) and (3.9) to (3.16), where it develops that P_3 vanishes.

6. Power of propulsion

Next we calculate the power available for propelling the hydrofoil through the fluid. By employing (4.9) and the notations given by (5.1), there follows

$$\mathscr{P}(t) = \frac{U}{b} \int_0^{2\pi} R_j(\Pi_1 + \Pi_2 + \Pi_3) 2 \sum_{n=1}^{\infty} \bar{c}_n' \sin n\theta \, d\theta - UR_i i \iint_{\mathscr{S}_B} R_j(\Pi_1 + \Pi_2 + \Pi_3) dz. \tag{6.1}$$

As was done previously, we calculate the power of propulsion in three parts depending upon the pressure terms Π_1, Π_2 or Π_3.

By using (5.1), (6.1) and (3.4) and by introducing the relation

$$\frac{\sin\theta}{|f'(be^{i\theta})|^2} 2 \sum_{n=1}^{\infty} c_n \sin n\theta = \gamma_0 + 2 \sum_{n=1}^{\infty} \gamma_n \cos n\theta \tag{6.2}$$

and by noting that the contour integral vanishes for a symmetric profile, the propulsive power resulting from the linearized non-circulatory flow becomes

$$\mathscr{P}_1(t) = -2\pi\rho \frac{U^3}{b}\left\{2 \sum_{n=1}^{\infty}\left[\sigma \frac{\bar{P}_n'' \bar{c}_n'}{n} + \bar{P}_n' \bar{\gamma}_n'\right]\right\}. \tag{6.3}$$

Similarly, by (5.1), (6.1) and (3.6), the propulsive power produced by the linearized circulatory flow is

$$\mathscr{P}_2(t) = R_j \frac{\rho U^3}{b} 2 \sum_{m=1}^{\infty} P_m e^{j\omega t} \int_0^{2\pi} \mathscr{W} 2 \sum_{n=1}^{\infty} \bar{c}_n' \sin n\theta \, d\theta, \tag{6.4}$$

where again it can be shown that the contour integral in (6.1) vanishes for a symmetric body. The integral in (6.4) is of the same type occurring in the previous section. After following the same integration procedure outlined there, together with the relations defined in (5.9), we obtain

$$\mathscr{P}_2(t) = 2\pi\rho\frac{U^3}{b}\Big\{2\sum_{m=1}^{\infty}\bar{P}'_m\Big[2\sum_{n=1}^{\infty}\bar{c}'_nU'+\bar{\gamma}'_0V'_0+2\sum_{n=1}^{\infty}\bar{\gamma}'_nV'_n\Big] - 2\sum_{m=1}^{\infty}\bar{P}''_m\Big[2\sum_{n=1}^{\infty}\bar{c}'_nU''_n+\bar{\gamma}'_0V''_0+2\sum_{n=1}^{\infty}\bar{\gamma}'_nV''_n\Big]\Big\}. \tag{6.5}$$

Finally, the contribution to the power of propulsion due to the pressure distribution Π_3 is given by (6.1) as

$$\mathscr{P}_3(t) = \frac{U}{b}\int_0^{2\pi}R_j\Pi_3 2\sum_{n=1}^{\infty}\bar{c}'_n\sin n\theta\,d\theta - R_i i\oiint_{\mathscr{S}_B}R_j\Pi_3 U\,dz. \tag{6.6}$$

If we recall that Π_3 is an even function of θ, then it can be shown that the first integral in the above equation vanishes. The remaining integral can most readily be calculated by a change of variable to the ζ-plane and by performing the corresponding contour integration around the circle of radius b. By using (3.9) and making the change of variable to the ζ-plane, we obtain

$$\mathscr{P}_3(t) = \tfrac{1}{4}\rho U R_i i\oint_{\mathscr{C}}[R_j(\hat{w}_1(\zeta,t)+\hat{w}_2(\zeta,t))]^2\frac{d\zeta}{f'(\zeta)}, \tag{6.7}$$

where $\mathscr{C}$ is the contour of the circle. Thus, by the residue theorem, it develops that

$$\mathscr{P}_3(t) = \tfrac{1}{2}\pi\rho U(b-\epsilon)\{R_j[\hat{w}_1(-b+2\epsilon,t)+\hat{w}_2(-b+2\epsilon,t)]\}^2. \tag{6.8}$$

Now we must evaluate $\hat{w}_1(-b+2\epsilon,t)$ and $\hat{w}_2(-b+2\epsilon,t)$. From the complex potential $F_1(\zeta,t)$ as given by (2.8), there follows after some straightforward manipulations

$$\hat{w}_1(b\mu,t) = \overline{\frac{\partial F_1}{\partial\zeta}}\bigg|_{\zeta=b\mu} = -iU e^{j\omega t}2\sum_{n=1}^{\infty}P_n(\mu)^{n-1}, \tag{6.9a}$$

where

$$\mu = -1+2\epsilon/b. \tag{6.9b}$$

Similarly, from the potential $F_2(\zeta,t)$ as given by (2.9), it can be shown that

$$\hat{w}_2(b\mu,t) = \overline{\frac{\partial F_2}{\partial\zeta}}\bigg|_{\zeta=b\mu} = -\frac{i\gamma_0 e^{j\omega t}}{2\pi b\mu}\int_b^{\infty}\Big[1+\sum_{n=1}^{\infty}\nu_n\Big(\frac{\xi_0}{b}\Big)^{-n}\Big]e^{-j\omega\tau}f'(\xi_0)\,d\xi_0, \tag{6.10a}$$

where

$$\nu_n = \mu^n+\frac{1}{\mu^n}. \tag{6.10b}$$

Then, from (2.10), (3.8), (3.13) and (3.15) there follows:

$$\hat{w}_2(b\mu,t) = -iU2\sum_{n=1}^{\infty}P_n e^{j\omega t}\frac{1}{\mu}\Big[V_0+\sum_{m=1}^{\infty}V_n\nu_n\Big]. \tag{6.11}$$

Finally, from (6.10), (6.12) and (6.9), we obtain

$$\mathscr{P}_3(t) = \frac{\pi\rho U^3(b-\epsilon)}{2\mu^2}\Big[2\sum_{m=1}^{\infty}\bar{P}'_n\mu^n+2\sum_{m=1}^{\infty}\bar{P}'_m\Big(V'_0+\sum_{n=1}^{\infty}V'_n\nu_n\Big) - 2\sum_{m=1}^{\infty}\bar{P}''_m\Big(V''_0+\sum_{n=1}^{\infty}V''_n\nu_n\Big)\Big]^2. \tag{6.12}$$

7. Input power, energy dissipation, and power of propulsion coefficients

As has been done in previous works, it is convenient to express the results in coefficient form. Therefore we define the following coefficients.

Power of propulsion or thrust coefficient:

$$C_T = C_T^{(1)} + C_T^{(2)} + C_T^{(3)}, \tag{7.1}$$

where
$$C_T^{(i)} = \frac{1}{\pi\rho U^3 T_0}\int_0^{T_0} \mathscr{P}_i(t)\,dt \quad (i = 1, 2, 3). \tag{7.2}$$

Input power coefficient:
$$C_P = C_P^{(1)} + C_P^{(2)} + C_P^{(3)}, \tag{7.3}$$

where
$$C_P^{(i)} = \frac{1}{\pi\rho U^3 T_0}\int_0^{T_0} P_i(t)\,dt \quad (i = 1, 2, 3). \tag{7.4}$$

Energy dissipation coefficient:

$$C_E = C_E^{(1)} + C_E^{(2)} + C_E^{(3)}, \tag{7.5}$$

where
$$C_E^{(i)} = C_P^{(i)} - C_T^{(i)} \quad (i = 1, 2, 3). \tag{7.6}$$

From (5.1) we can perform the indicated time integration by noting that

$$\frac{1}{T_0}\int_0^{T_0} \bar{b}_n' \bar{P}_n' = \tfrac{1}{2}(b_n' P_n' + b_n'' P_n'') \tag{7.7a}$$

and
$$\frac{1}{T_0}\int_0^{T_0} \bar{b}_n' \bar{P}_n'' = \tfrac{1}{2}(b_n' P_n'' - b_n'' P_n') \tag{7.7b}$$

and similar relationships for the integral of other products.

By substituting the results of (6.3), (6.5), (6.12) and (7.7) into (7.2), we obtain the following.

Non-circulatory thrust coefficient:

$$C_T^{(1)} = -\frac{1}{b}\sum_{n=1}^{\infty}\left[\sigma\frac{P_n'' c_n' - P_n' c_n''}{n} + P_n'\gamma_n' + P_n''\gamma_n''\right]. \tag{7.8}$$

Circulatory thrust coefficient:

$$\begin{aligned} C_T^{(2)} = \frac{1}{b}\sum_{n=1}^{\infty}\Bigg\{ \sum_{m=1}^{\infty} [&2(P_m' c_n' + P_m'' c_n'')U_n' - 2(P_m'' c_n' - P_m' c_n'')U_n'' \\ &+ (P_m'\gamma_0' + P_m''\gamma_0'')V_0' + 2(P_m'\gamma_n' + P_m''\gamma_n'')\,V_n' - (P_m''\gamma_0' - P_m'\gamma_0'')V_0'' \\ &- 2(P_m''\gamma_n' - P_m'\gamma_n'')V_n''] \Bigg\}, \end{aligned} \tag{7.9}$$

and the non-linear contribution to the thrust coefficient

$$\begin{aligned} C_T^{(3)} = \frac{b-e}{2\mu^2}\Bigg\{ \sum_{n=1}^{\infty}\Bigg[&(P_n' + P_n'')\left(\mu^n + V_0' + \sum_{m=1}^{\infty} V_m'\nu_m\right) \\ &+ (P_n' - P_n'')\left(V_0'' + \sum_{m=1}^{\infty} V_m''\nu_m\right)\Bigg]\Bigg\}^2. \end{aligned} \tag{7.10}$$

Further, from (7.4), (5.4), (5.10) and (7.7) there follows

Non-circulatory input power coefficient:

$$C_P^{(1)} = \frac{\sigma}{b}\sum_{n=1}^{\infty}\left(\sigma\frac{P_n' b_n' + P_n'' b_n''}{n} + P_n'\beta_n'' - P_n''\beta_n'\right). \tag{7.11}$$

Circulatory input power coefficient:

$$C_P^{(2)} = \frac{\sigma}{b}\sum_{n=1}^{\infty}\left\{\sum_{m=1}^{\infty}[2(P'_m b'_n + P''_m b''_n)U''_n + 2(P''_m b'_n - P'_m b''_n)U'_n + (P'_m\beta'_0 + P''_m\beta''_0)V''_0 + 2(P'_m\beta'_n + P''_m\beta''_n)V''_n + (P''_m\beta'_0 - P'_m\beta''_0)V'_0 + 2(P''_m\beta'_n - P'_m\beta''_n)V'_n]\right\} \quad (7.12)$$

and

$$C_P^{(3)} = 0. \quad (7.13)$$

The energy dissipated in the wake can be determined quite simply by (7.5). Finally, we can compute the gross theoretical hydrodynamic efficiency by

$$\eta_{\text{eff}} = \frac{\text{power of propulsion}}{\text{input power}} \times 100, \quad (7.14)$$

or

$$\eta_{\text{eff}} = \frac{C_T}{C_P} \times 100. \quad (7.15)$$

8. Numerical analysis and example

In order to determine numerical values for the various coefficients above, it is necessary to compute the real and imaginary parts of the b_n, β_n, c_n and γ_n coefficients and the real and imaginary parts of the wake functions U_n and V_n. Once the b_n and c_n coefficients are known, the P_n coefficients can be found rather simply by using (2.7).

From (2.6), (2.7), (5.4) and the Fourier inversion formula, there follows

$$b_n = -\frac{1}{\pi}\int_0^{\pi}\frac{dx}{d\theta}H^*(x)\sin n\theta\, d\theta \quad (8.1)$$

and

$$\beta_n = -\frac{1}{\pi}\int_0^{\pi}\frac{\sin\theta}{|f'(b\,e^{i\theta})|^2}\frac{dx}{d\theta}H^*(x)\cos n\theta\, d\theta. \quad (8.2)$$

In order to compare this theory with that of previous authors, we take a quadratic displacement function as

$$H^*(x) = (d_0 + d_1 x + d_2 x^2)e^{-j\alpha x} \quad (-L \leqslant x \leqslant L), \quad (8.3)$$

where the d_i's are taken from observations of the swimming of certain types of sea animals, x is the abscissa of points on the stretched-straight hydrofoil measured from the centre, and α is the wave-number.

Thus, from (2.2) we have

$$x = \tfrac{1}{2}(b\cos\theta - \epsilon)\left(1 - \frac{(b-\epsilon)^2}{b^2+\epsilon^2-2b\epsilon\cos\theta}\right) + E, \quad (8.4)$$

where

$$E = L - b + \epsilon. \quad (8.5)$$

With the aid of these last results and (8.1) to (8.3), we find the real and imaginary parts of the b_n and β_n coefficients to be

$$b'_n + jb''_n = -\frac{1}{\pi}\int_0^{\pi}\frac{dx}{d\theta}(d_0 + d_1 x + d_2 x^2)e^{-j\alpha x}\sin n\theta\, d\theta \quad (8.6)$$

and

$$\beta'_n + j\beta''_n = -\frac{1}{\pi}\int_0^{\pi}\frac{\sin\theta}{|f'(b\,e^{i\theta})|^2}\frac{dx}{d\theta}(d_0 + d_1 x + d_2 x^2)e^{-j\alpha x}\cos n\theta\, d\theta. \quad (8.7)$$

Similarly, from (2.8) to (2.10), (6.3) and (8.3), there follows

$$c_n'+jc_n''=\frac{1}{\pi}\int_0^{\pi}\left[\frac{\sin\theta}{|f'(be^{i\theta})|^2}\left(\frac{dx}{d\theta}\right)^2\right]\times[j\alpha(d_0+d_1x+d_2x^2)-(d_1+2d_2)]e^{-j\alpha x}\sin n\theta\,d\theta \tag{8.8}$$

and

$$\gamma_n'+j\gamma_n''=\frac{1}{\pi}\int_0^{\pi}\left[\frac{\sin\theta}{|f'(be^{i\theta})|^2}\frac{dx}{d\theta}\right]^2\times[j\alpha(d_0+d_1x+d_2x^2)-(d+2d_2)]e^{-j\alpha x}\cos n\theta\,d\theta. \tag{8.9}$$

All of the above displacement coefficients have been computed through $n=32$ by numerical integration techniques with the aid of an electronic digital computer for values of the thickness parameter $\epsilon=0{\cdot}1,\ 0{\cdot}2,\ 0{\cdot}3$.

Let us now consider the numerical analysis of the wake functions W_0, W_{1n} and W_{2n} as given by equations (3.8), (3.14) and (5.13), respectively, and in particular their ratios U_n and V_n as defined by (5.15) and (5.16). As can be seen, the integrands of these integrals oscillate an infinite number of times in the integration interval where the exponential involves the age of a vortex element τ. Since our theory is applicable only for relatively small values of the reduced frequency σ, say in the range $\sigma=0\to10$, we propose to employ a method of analysis similar to that used by Küssner & Gorup (1960).

By introducing a new variable defined by

$$u=b/\xi_0 \tag{8.10}$$

into equation (2.11) and by employing (2.2), the age of a vortex situated at $\xi_0=b/u$ becomes

$$\tau=-\frac{b}{2U}\int_1^u\frac{u^2}{1-u^2}\left[\frac{1}{u^2}-\left(\frac{b-\epsilon}{b-\epsilon u}\right)^2\right]^2du. \tag{8.11}$$

By using partial fractions and after some rather lengthy algebraic manipulations, (8.11) can be integrated analytically to yield

$$\tau=\frac{b}{2U}\left[\frac{1}{u}-1+\tau^*(u)\right], \tag{8.12}$$

where

$$\tau^*(u)=\tfrac{1}{2}(1-q^2)^2\log\frac{2}{r(1+u)}+\tfrac{1}{2}(1-2q+q^3)(1-r)-\tfrac{1}{4}(1-q^2)(1-r^2)-\tfrac{1}{6}(1-q)(1-r^3)-\frac{r(1-u)}{(b-\epsilon u)^2}\left[b^2-b\epsilon(1+u)+\frac{\epsilon^2}{3}(1+u+u^2)\right] \tag{8.13a}$$

in which

$$q=\frac{b-\epsilon}{b+\epsilon},\quad r=\frac{b-\epsilon}{b-\epsilon u}. \tag{8.13b}$$

Here $\tau^*(u)$ is a holomorphic function in our interval $u=0\to1$.

By making the change of variable defined by (8.10) and employing (2.2), equations (3.8), (5.7) and (3.13) become

$$W_0=\frac{1}{2}\int_0^1\frac{1+u}{1-u}(1-r^2u^2)\exp\left\{-j\chi\left(\frac{1}{u}-1\right)\right\}\exp\{-j\chi\tau^*\}\frac{du}{u^2}, \tag{8.14}$$

$$W_{1n}=\int_0^1\frac{1-u^2}{1-r^2u^2}(u)^{n+1}\exp\left\{-j\chi\left(\frac{1}{u}-1\right)\right\}\exp\{-j\chi\tau^*\}\frac{du}{u^2} \tag{8.15}$$

and $$W_{2n} = \frac{1}{2}\int_0^1 (1-r^2u^2)\,u^n \exp\left\{-j\chi\left(\frac{1}{u}-1\right)\right\}\exp\{-j\chi\tau^*\}\frac{du}{u^2}, \tag{8.16}$$

where $\chi = \frac{1}{2}\sigma$.

As can be seen, the factor $(1/u^2)\exp\{-j\chi(1/u)\}$ in the integrand of these integrals is singular and the remaining factors are regular functions in the integration interval. For values of $\sigma \leqslant 10$ we can expand these regular factors into polynomials of the form

$$P_i(u) = \sum_{n=0}^{\infty} \sigma_{in} u^n \quad (i = 0, 1, 2), \tag{8.17a}$$

where $$P_0(u) = \frac{1+u}{1-u}(1-r^2u^2)\exp\{-j\chi\tau^*(u)\}, \tag{8.17b}$$

$$P_1(u) = \frac{1-u^2}{1-r^2u^2}\exp\{-j\chi\tau^*(u)\} \tag{8.17c}$$

and $$P_2(u) = (1-r^2u^2)\exp\{-j\chi\tau^*(u)\}. \tag{8.17d}$$

Now, with the aid of these polynomials, the wake functions can be integrated analytically to give

$$W_0 = \frac{1}{2}\sum_{m=0}^{\infty} \sigma_{0m}\Sigma_m \frac{e^{j\chi}}{j\chi}, \tag{8.18}$$

$$W_{1n} = \sum_{m=0}^{\infty} \sigma_{1m}\Sigma_{m+n+1} \frac{e^{j\chi}}{j\chi}, \tag{8.19}$$

$$W_{2n} = \frac{1}{2}\sum_{m=0}^{\infty} \sigma_{2m}\Sigma_{m+n} \frac{e^{j\chi}}{j\chi}, \tag{8.20}$$

in which $$\Sigma_n = j\chi\int_0^1 u^{n-2}\exp\left(-j\frac{\chi}{u}\right)du. \tag{8.21}$$

By integrating (8.21) we obtain the results

$$\Sigma_0 = \Sigma_0' + j\Sigma_0'' = e^{-j\chi}, \tag{8.22a}$$

$$\Sigma_1 = \Sigma_1' + j\Sigma_2'' = -j\chi[\gamma^* + \log j\chi] + \sum_{n=1}^{\infty} \frac{(-j\chi)^{n+1}}{n\,n!}, \tag{8.22b}$$

where $\gamma^* = 0{\cdot}5772157$, Euler's constant, and

$$\Sigma_n = \Sigma_n' + j\Sigma_n'' = \frac{j\chi}{n-1}(e^{-j\chi} - \Sigma_{n-1}). \tag{8.22c}$$

In order to evaluate the σ_{in} coefficients, we first approximate $\tau^*(u)$ given by (8.13) by a 'least squares' fit with a second-degree polynomial of the form

$$\tau^*(u) \doteq A + Bu + Cu^2, \tag{8.23}$$

and then make the following series expansion:

$$\left.\begin{aligned} \frac{1+u}{1-u}(1-r^2u^2) = \sum_{n=0}^{\infty} \tilde{a}_n u^n, \quad \frac{1-u^2}{1-r^2u^2} = \sum_{n=0}^{\infty} \tilde{b}_n u^n, \\ 1-r^2u^2 = \sum_{n=0}^{\infty} \tilde{c}_n u^n, \end{aligned}\right\} \tag{8.24}$$

where with the aid of (8.13*b*) the $\tilde{a}_n$, $\tilde{b}_n$ and $\tilde{c}_n$ can be found quite easily.

Now we expand the exponential function in a MacLaurin power series as

$$\exp\{-j\chi\tau^*(u)\} = \sum_{n=0}^{\infty} [\tilde{\delta}_n \cos\chi A - \tilde{\lambda}_n \sin\chi A - j(\tilde{\delta}_n \sin\chi A + \tilde{\lambda}_n \cos\chi A)]u^n, \qquad (8.25)$$

where, after some tedious algebra, the coefficients $\tilde{\delta}_n$ and $\tilde{\lambda}_n$ can be found to depend upon B, C and χ.

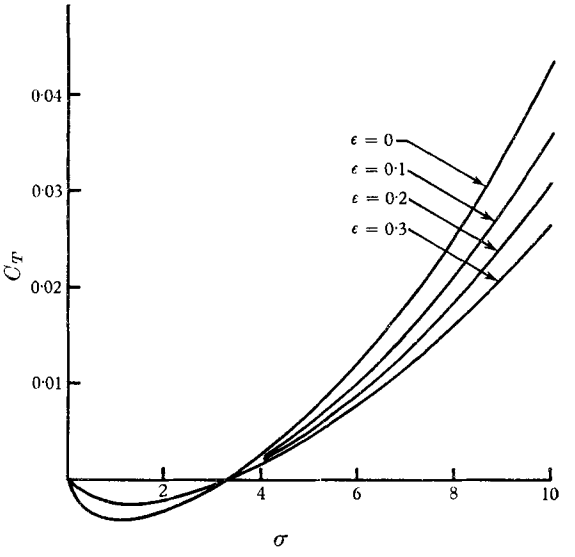

FIGURE 2. Thrust coefficient *vs.* reduced frequency ($\alpha = \pi$).

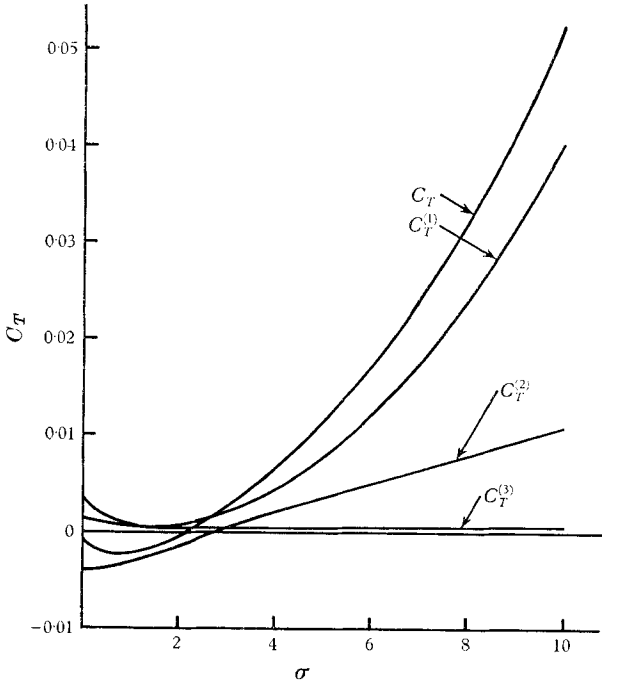

FIGURE 3. Thrust coefficient *vs.* reduced frequency ($\alpha = \frac{1}{2}\pi$, $\epsilon = 0{\cdot}2$).

From (8.13), $\tau^*(u)$ was calculated for eleven equally spaced values of u running from 0 to 1·0 and for values of ϵ of 0, 0·1, 0·2 and 0·3. Next, by employing a standard least squares technique, the constants A, B and C in equation (8.23) were computed. Then, for the numerical calculations of the real and imaginary parts

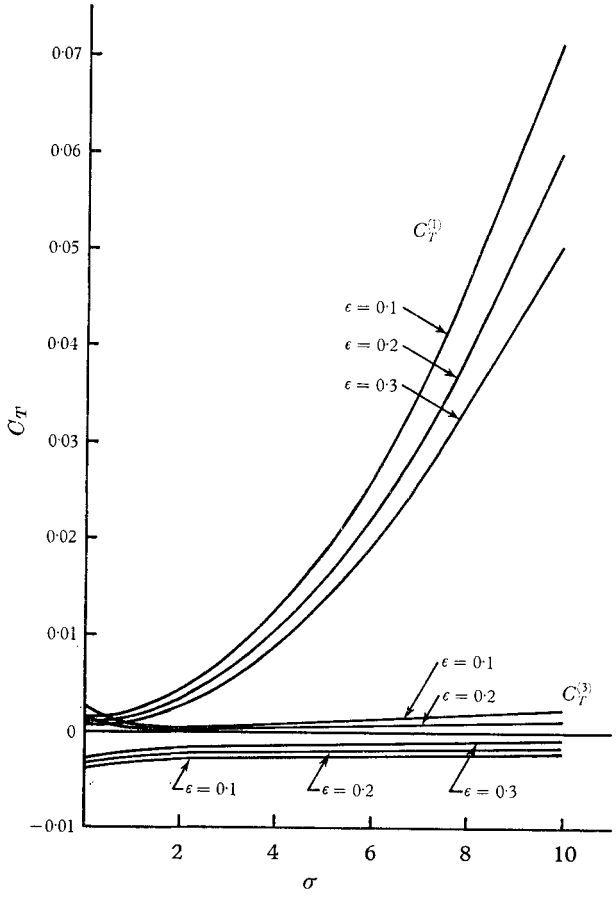

FIGURE 4. Thrust coefficient *vs.* reduced frequency ($\alpha = 0$).

of the wake functions V'_n, V''_n, U'_n and U''_n equations (8.18), (8.19), (8.20), (8.22), (8.24), (8.25), (5.15) and (5.16) were programmed and calculations performed for the different values of the thickness parameter ϵ given above and for reduced frequencies $\sigma = 0$, 1, 2, 4, 6, 8 and 10. In order to obtain accuracy to the fifth place in the thrust and power coefficients, it was necessary to compute $n = 32$ wake functions for each thickness parameter and each reduced frequency.

Finally, (7.8) to (7.13) were programmed for the numerical calculations of the various thrust and power coefficients. These results are given in tables 1 to 3. Some of the significant results are plotted in figures 2 to 11.

Shown in figure 2 is the effect of thickness on the thrust coefficient for a wavenumber, $\alpha = \pi$. Figure 3 shows the contributions to the total thrust by the non-circulatory flow, the circulatory flow, and the non-linear pressure distribution

on the body. In figure 4 is shown the effect of both thickness and magnitude of the thrust generated by the non-circulatory flow, the circulatory flow, and the non-linear pressure distribution on the body for a standing-wave-type swimming

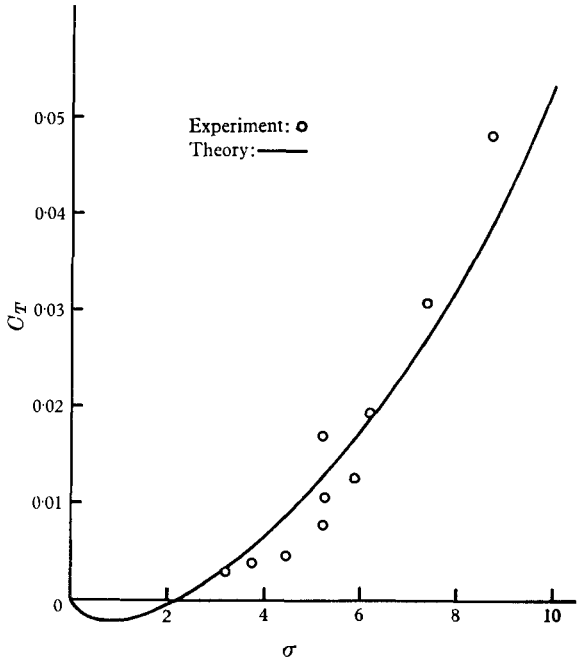

FIGURE 5. Thrust coefficient *vs.* reduced frequency ($\alpha = \frac{1}{2}\pi$, $\epsilon = 0{\cdot}2$).

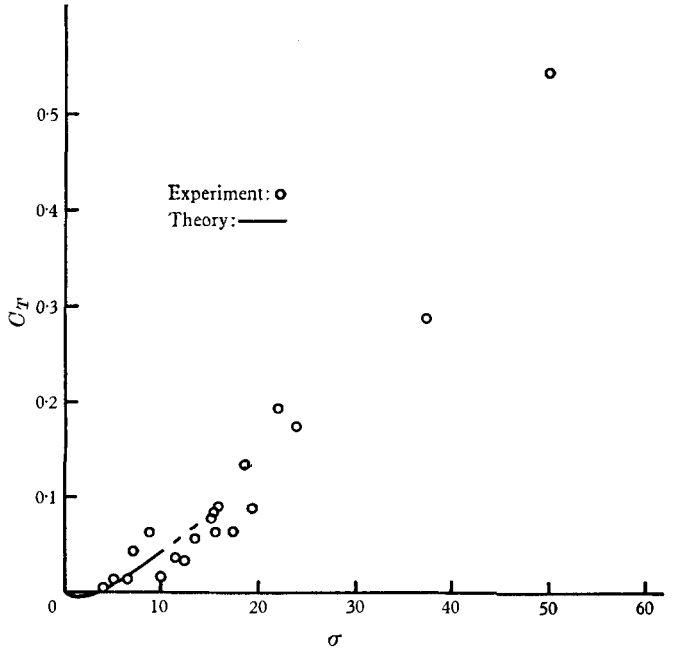

FIGURE 6. Thrust coefficient *vs.* reduced frequency ($\alpha = \frac{1}{2}\pi$, $\epsilon = 0{\cdot}3$).

motion. It should be noted that with a standing-wave swimming motion the wake produces no net forward thrust, whereas for a finite wave speed such as is depicted in figure 3 the wake produces a net forward thrust for sufficiently large reduced frequencies.

Shown in figures 5 and 6 are some recent experimental results obtained in the engineering mechanics laboratories at Clemson University using flexible hydrofoils of finite thickness moulded with a Silastic RTV Silicone rubber, the shape of the profiles being that given by the present theory.

In interpreting these results, it must be kept in mind that the present theory is based on unsteady airfoil theory wherein it is assumed that the inertia forces play the predominant role in generating propulsion and the viscous effect is only responsible for generation of the wake by requiring smooth attached flow

	$C_T^{(1)}$	$C_T^{(2)}$	$C_T^{(3)}$	$C_P^{(1)}$	$C_P^{(2)}$	C_T	C_P	η_{eff} (%)
				$\epsilon = 0{\cdot}1,\ \alpha = \pi$				
0	0·00369	−0·00646	0·00277	0	0	0	0	—
1	0·00178	−0·00549	0·00005	−0·00011	−0·00152	−0·00366	−0·00163	—
2	0·00069	−0·00341	0·00005	−0·00013	−0·00151	−0·00267	−0·00164	—
4	0·00094	0·00109	0·00009	0·00010	0·00295	0·00212	0·00305	69·5
6	0·00442	0·00562	0·00013	0·00071	0·01331	0·01017	0·01402	72·8
8	0·01115	0·01019	0·00017	0·00169	0·02960	0·02151	0·03129	68·8
10	0·02120	0·01462	0·00024	0·00302	0·05090	0·03606	0·05392	67·2
				$\epsilon = 0{\cdot}1,\ \alpha = \frac{1}{2}\pi$				
0	0·00194	−0·00577	0·00383	0	0	0	0	—
1	0·00092	−0·00337	0·00031	−0·00003	−0·00065	−0·00213	−0·00068	—
2	0·00111	−0·00127	0·00007	0·00007	0·00100	−0·00009	0·00108	—
4	0·00509	0·00253	0·00006	0·00071	0·01124	0·00768	0·01195	64·2
6	0·01391	0·00621	0·00025	0·00190	0·03068	0·02037	0·03258	62·6
8	0·02754	0·00982	0·00059	0·00366	0·05925	0·03797	0·06292	60·4
10	0·04601	0·01340	0·00109	0·00598	0·09694	0·06051	0·10292	58·7
				$\epsilon = 0{\cdot}1,\ \alpha = 0$				
0	0·00114	−0·00300	0·00187	0	0	0	0	—
1	0·00184	−0·00251	0·00030	0·00006	0·00138	−0·00036	0·00146	—
2	0·00394	−0·00239	0·00044	0·00028	0·00584	0·00199	0·00612	32·5
4	0·01236	−0·00224	0·00114	0·00115	0·02354	0·01126	0·02470	45·7
6	0·02637	−0·00212	0·00234	0·00258	0·05289	0·02659	0·05547	48·0
8	0·04601	−0·00201	0·00401	0·00459	0·09378	0·04801	0·09838	48·8
10	0·07124	−0·00191	0·00617	0·00717	0·14618	0·07551	0·15336	49·4

TABLE 1. Thrust and power input coefficients, C_T and C_P. $d_0 = 0{\cdot}023$, $d_1 = 0{\cdot}042$, $d_2 = 0{\cdot}034$.

at the tail. Therefore, in order to compare the theory realistically with experimental observations, an attempt was made to separate the effect of frictional drag and the effect of the unsteady thrust produced by the swimming motion of the hydrofoil. This was done by measuring the frictional drag at a prescribed forward speed with no undulations imposed upon the hydrofoil, and then measuring the thrust generated for various driving frequencies, ω, at the same forward speed of the hydrofoil and separating the steady-state streamwise force

from the time average unsteady streamwise thrusts. This procedure allowed the measurement of several thrust coefficients for the several reduced frequencies at only one forward speed. Of course this technique assumes that there is no interaction between the unsteady undulations and the development of the boundary layer. Further experimental and analytical investigation into this phenomenon is needed.

	$C_T^{(1)}$	$C_T^{(2)}$	$C_T^{(3)}$	$C_P^{(1)}$	$C_P^{(2)}$	C_T	C_P	η_{eff} (%)
				$\epsilon = 0{\cdot}2,\ \alpha = \pi$				
0	0·00278	−0·00413	0·00134	0	0	0	0	—
1	0·00122	−0·00437	0·00003	−0·00018	−0·00119	−0·00310	−0·00137	—
2	0·00038	−0·00277	0·00003	−0·00021	−0·00117	−0·00236	−0·00138	—
4	0·00082	0·00087	0·00004	0·00013	0·00249	0·00175	0·00263	66·6
6	0·00410	0·00457	0·00006	0·00105	0·01090	0·00875	0·01196	73·2
8	0·01024	0·00823	0·00009	0·00254	0·02401	0·01856	0·02657	69·7
10	0·01921	0·01184	0·00011	0·00461	0·04179	0·03118	0·04641	67·2
				$\epsilon = 0{\cdot}2,\ \alpha = \frac{1}{2}\pi$				
0	0·00146	−0·00503	0·00358	0	0	0	0	—
1	0·00067	−0·00307	0·00027	0·00006	−0·00056	−0·00211	−0·00061	—
2	0·00091	−0·00120	0·00007	0·00009	·000077	−0·00021	0·00086	—
4	0·00455	0·00204	0·00004	0·00106	0·00903	0·00665	0·01009	65·8
6	0·01235	0·00512	0·00017	0·00289	0·02465	0·01765	0·02755	64·2
8	0·02434	0·00809	0·00042	0·00558	0·04755	0·03285	0·05315	61·8
10	0·04050	0·01100	0·00077	0·00914	0·07768	0·05227	0·08683	60·4
				$\epsilon = 0{\cdot}2,\ \alpha = 0$				
0	0·00088	−0·00285	0·00196	0	0	0	0	—
1	0·00148	−0·00217	0·00026	0·00011	0·00112	−0·00042	0·00123	—
2	0·00327	−0·00197	0·00034	0·00044	0·00476	0·00165	0·00521	31·7
4	0·01044	−0·00169	0·00086	0·00180	0·01914	0·00962	0·02095	46·2
6	0·02240	−0·00147	0·00178	0·00406	0·04281	0·02269	0·04689	48·4
8	0·03914	−0·00129	0·00306	0·00723	0·07566	0·04090	0·08289	49·4
10	0·06065	−0·00113	0·00471	0·01129	0·11760	0·06423	0·12891	50·1

TABLE 2. Thrust and power input coefficients, C_T and C_P. $d_0 = 0{\cdot}023$, $d_1 = 0{\cdot}042$, $d_2 = 0{\cdot}034$.

Figures 7 and 8 indicate how the wave-number and thickness affect the power input coefficients. Figure 9 shows the necessary power required to generate the non-circulatory flow and the wake. It should be noted that a large percentage of the input power is used in the generation of the wake.

Finally, in figures 10 and 11 are shown the resulting hydrodynamic efficiency for various swimming motions and thicknesses.

9. Conclusion

In the present analysis an attempt has been made to gain a better fundamental understanding of the mechanics of swimming of flexible bodies. By employing a two-dimensional flexible hydrofoil of finite thickness for the model of the swimmer and solving the unsteady potential flow problem by resolving it

nto the non-circulatory and circulatory flows around the body, several interesting observations can be made. Following are some of the significant results.

(i) The input power required to drive the hydrofoil and the resulting power of propulsion both decrease with increasingly thick profiles. This effect is more pronounced at larger reduced frequencies than at smaller ones.

	$C_T^{(1)}$	$C_T^{(2)}$	$C_T^{(3)}$	$C_P^{(1)}$	$C_P^{(2)}$	C_T	C_P	η_{eff} (%)
				$\epsilon = 0{\cdot}3,\ \alpha = \pi$				
0	0·00208	−0·00222	0·00014	0	0	0	0	—
$\frac{1}{2}$	0·00135	−0·00361	0·00001	−0·00013	−0·00060	−0·00224	−0·00073	—
1	0·00079	−0·00346	0	−0·00023	−0·00095	−0·00267	−0·00118	—
2	0·00013	−0·00224	0	−0·00027	−0·00088	−0·00211	−0·00117	—
4	0·00071	0·00077	0	0·00013	0·00220	0·00149	0·00233	63·8
6	0·00383	0·00382	0	0·00124	0·01914	0·00765	0·01038	74
8	0·00946	0·00679	0·00001	0·00304	0·01990	0·01627	0·02294	71·1
				$\epsilon = 0{\cdot}3,\ \alpha = \frac{1}{2}\pi$				
0	0·00106	−0·00441	0·00335	0	0	0	0	—
$\frac{1}{2}$	0·00064	−0·00382	0·00064	−0·00006	−0·00044	−0·00255	−0·00052	—
1	0·00044	−0·00275	0·00024	−0·00007	−0·00048	−0·00206	−0·00056	—
2	0·00074	−0·00107	0·00006	0·00010	0·00061	−0·00027	0·00072	—
4	0·00408	0·00174	0·00003	0·00125	0·00739	0·00586	0·00864	67·8
6	0·01107	0·00433	0·00013	0·00345	0·02014	0·01554	0·02359	65·9
8	0·02172	0·00678	0·00031	0·00669	0·03873	0·02884	0·04543	63·4
				$\epsilon = 0{\cdot}3,\ \alpha = 0$				
0	0·00066	−0·00273	0·00207	0	0	0	0	—
$\frac{1}{2}$	0·00079	−0·00208	0·00036	0·00003	0·00017	−0·00091	0·00020	—
1	0·00118	−0·00184	0·00023	0·00014	0·00091	−0·00042	0·00104	—
2	0·00273	−0·00157	0·00028	0·00055	0·00392	0·00144	0·00446	32·3
4	0·00893	−0·00120	0·00071	0·00220	0·01573	0·00844	0·01840	45·9
6	0·01928	−0·00091	0·00146	0·00496	0·03505	0·01982	0·04003	49·5
8	0·03375	−0·00068	0·00253	0·00884	0·06171	0·03560	0·07056	50·6

TABLE 3. Thrust and power input coefficients, C_T and C_P. $d_0 = 0{\cdot}023$, $d_1 = 0{\cdot}042$, $d_2 = 0{\cdot}034$.

(ii) A high percentage of the power of propulsion is derived from the non-circulatory flow around the hydrofoil.

(iii) The wake produces no net forward thrust for a standing-wave-type swimming motion, whereas for finite displacement wave velocities the wake can produce positive propulsion for certain reduced frequencies.

(iv) The thrust produced by the non-linear unsteady perturbation velocities in the Bernoulli equation is positive for all values of the reduced frequencies. However, this thrust is quite small compared with the linear terms except for very small reduced frequencies.

(v) A very high proportion of the input power is used in the generation of the wake vortices.

(vi) High swimming efficiencies are associated with high wave-numbers. For the type of swimming motion used in the present analysis, the maximum hydrodynamic efficiency was approximately 74 % with a wave-number equal to π and a reduced frequency of 6. For this efficiency, the corresponding displacement wave velocity is approximately 90 % greater than the forward speed of the swimmer

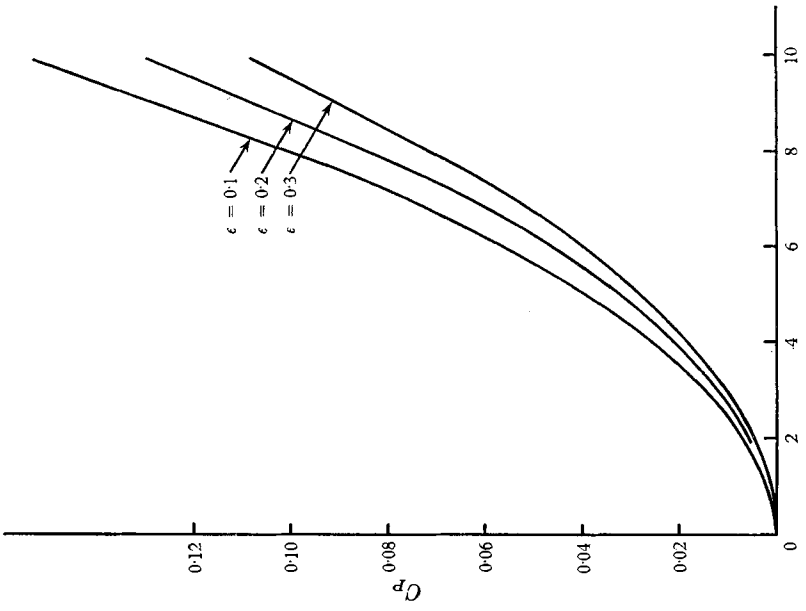

FIGURE 8. Power coefficients *vs.* reduced frequency ($\alpha = 0$).

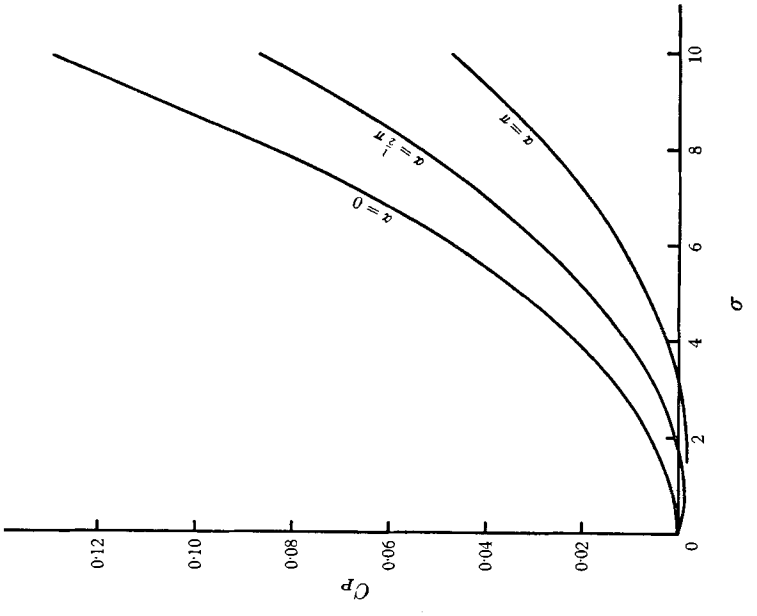

FIGURE 7. Power coefficients *vs.* reduced frequency ($\epsilon = 0{\cdot}2$).

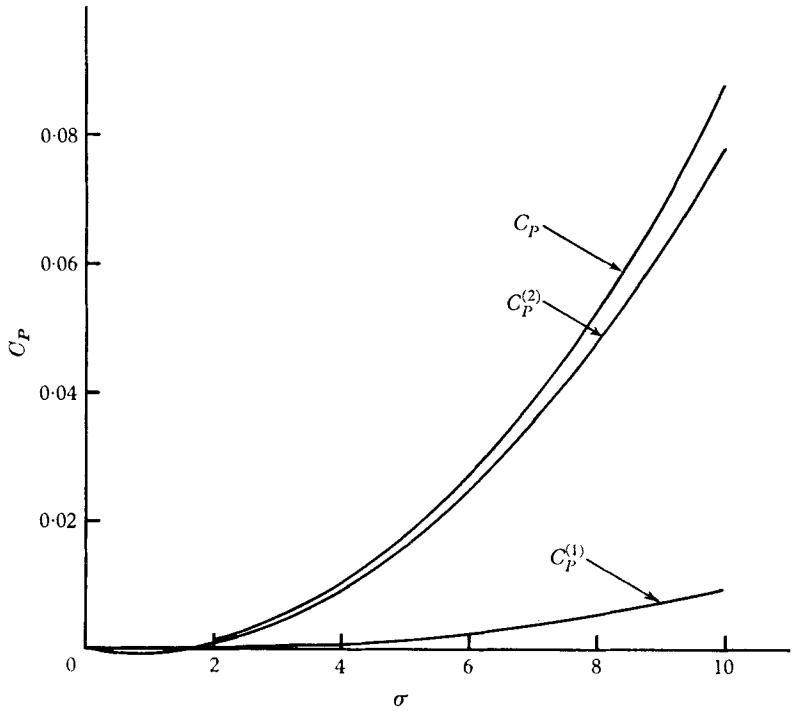

Figure 9. Power coefficients *vs.* reduced frequency ($\alpha = \pi/2$).

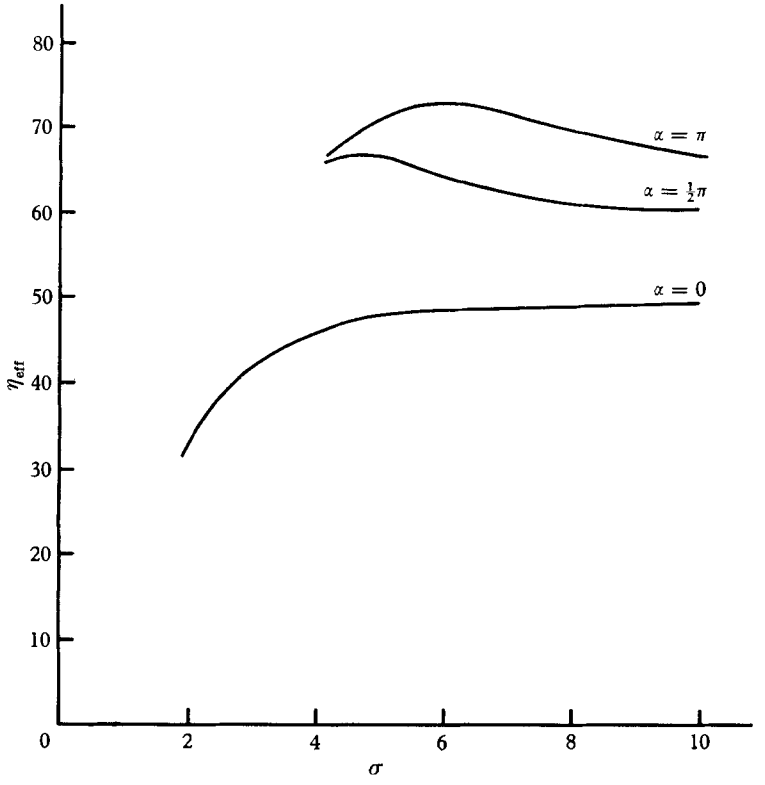

Figure 10. Efficiency *vs.* reduced frequency ($\epsilon = 0{\cdot}2$).

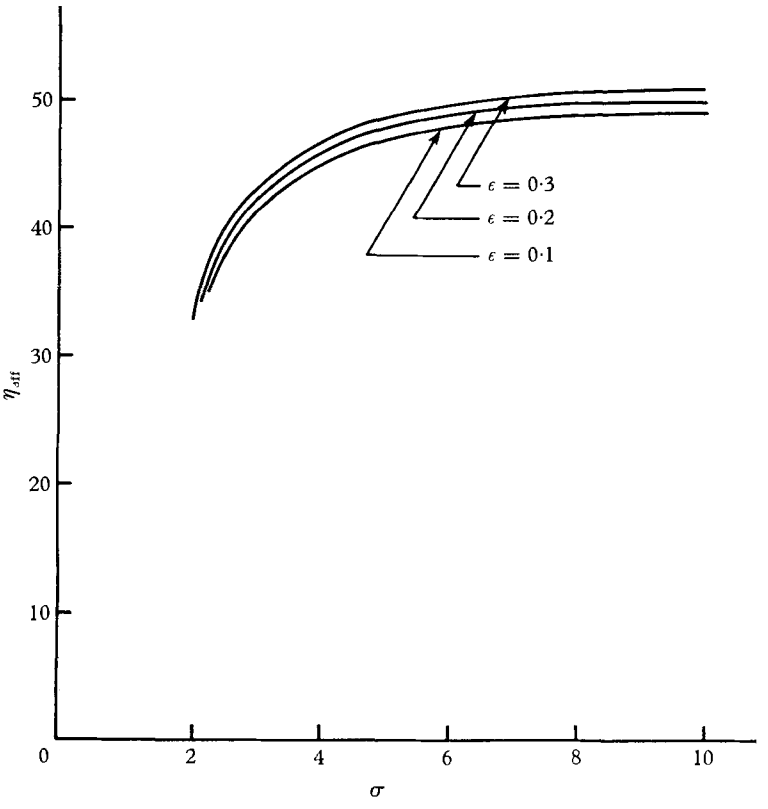

Figure 11. Efficiency *vs.* reduced frequency ($\alpha = 0$).

This research was sponsored by the National Science Foundation under contract no. G-3030.

REFERENCES

BONTHRON, R. J. & FEJER, A. A. 1962 A hydrodynamic study of fish locomotion. *Proc. 4th U.S. Nat. Congr. Appl. Mech.* pp. 1249–55. Berkeley, California.

GRAY, J. 1936 Studies of animal locomotion. VI. *J. Exp. Biol.* **13**, 192–9.

GRAY, J. 1948 Aspects of locomotion of whales. *Nature, Lond.* **161**, 191–200.

GRAY, J. 1957 How fish swim. *Sci. Am.* **197**, 48–54.

KELLY, H. R. 1961 Fish propulsion hydrodynamics. *Proc. 7th Midwestern Conf. on Fluid Mech.*, Michigan State University. In *Developments in Mechanics*, **1**, 442–50. New York: Plenum Press.

KELLY, H. R. & BOWLUS, G. H. 1963 Swimming hinged hydrofoils. *NAVWEPS Rept. NOTS TP* 3342, China Lake, California.

KÜSSNER, H. G. & GORUP, G. V. 1960 Instationäre linearisierte Theorie der Flügelprofile endlicher Diche in inkompressibler Strömung. *Mitt. Max-Planck-Institut Ström. Forsch.* **26**, Göttingen.

KÜSSNER, H. G. & SCHWARZ, L. 1940 The oscillating wing with aerodynamically balanced elevator. *Luftfahrforschung*, **17**, 337–54. English translation 1941: *N.A.C.A.* T.M. 991.

LIGHTHILL, M. J. 1960*a* Mathematics and aeronautics. *J. Roy. Aero. Soc.* **64**, 373–94.

LIGHTHILL, M. J. 1960*b* Note on the swimming of slender fish. *J. Fluid Mech.* **9**, 305–17.

MUNK, M. M. 1924 The aerodynamic forces on airship hulls. *N.A.C.A. Tech. Rept.* no. 184.

PAO, S. K. & SIEKMANN, J. 1964 Note on the Smith–Stone theory of fish propulsion. *Proc. Roy. Soc.* A **280**, 398–408.

SCHWARZ, L. 1940 Berechnung der Druckverteilung einer harmonich sich verformenden Tragfläche in ebener Strömung. *Luftfahrforschung*, **17**, 379–86.

SERRIN, J. 1959 Mathematical principles of classical fluid mechanics. *Handbuch der Physik* VIII/1.

SIEKMANN, J. 1962 Theoretical studies of sea animal locomotion, Part I. *Ing. Arch.* Bd. 31, H. 3, 214–28.

SIEKMANN, J. 1963*a* Theoretical studies of sea animal locomotion. Part II. *Ing. Arch.* Bd. 32, H.1, 40–50.

SIEKMANN, J. 1963*b* On a pulsating jet from the end of a tube, with application to the propulsion of certain aquatic animals. *J. Fluid Mech.* **15**, 399–418.

SMITH, E. H. & STONE, D. E. 1961 Perfect fluid forces in fish propulsion: the solution of the problem in an elliptic cylinder coordinate system. *Proc. Roy. Soc.* A **261**, 316–28.

TAYLOR, G. 1951 Analysis of the swimming of microscopic organisms. *Proc. Roy. Soc.* A **209**, 445.

TAYLOR, G. 1952*a* The action of waving cylindrical tails in propelling microscopic organisms. *Proc. Roy. Soc.* A **211**, 225–39.

TAYLOR, G. 1952*b* Analysis of the swimming of long and narrow animals. *Proc. Roy. Soc.* A **214**, 158–83.

THEODORSEN, T. 1934 General theory of aerodynamic instability and the mechanism of flutter. *N.A.C.A. Rept.* no. 496.

ULDRICK, J. P. & SIEKMANN, J. 1964 On the swimming of a flexible plate of arbitrary finite thickness. *J. Fluid Mech.* **20**, 1–33.

WU, T. Y. 1961 Swimming of a waving plate. *J. Fluid Mech.* **10**, 321–44.